MULTISCALE MODEL. SIMUL.
Vol. 11, No. 1, pp. 118–133

CDF SOLUTIONS OF BUCKLEY–LEVERETT EQUATION WITH UNCERTAIN PARAMETERS*

P. WANG†, D. M. TARTAKOVSKY‡, K. D. JARMAN, JR.†, AND A. M. TARTAKOVSKY†

Abstract. The Buckley–Leverett (nonlinear advection) equation is often used to describe two-phase flow in porous media. We develop a new probabilistic method to quantify parametric uncertainty in the Buckley–Leverett model. Our approach is based on the concept of a fine-grained cumulative density function (CDF) and provides a full statistical description of the system states. Hence, it enables one to obtain not only average system response but also the probability of rare events, which is critical for risk assessment. We obtain a closed-form, semianalytical solution for the CDF of the state variable (fluid saturation) and test it against the results from Monte Carlo simulations.

Key words. uncertainty quantification, Buckley–Leverett equation, multiphase flow, probability density function, cumulative density function, oil recovery

AMS subject classifications. 15A15, 15A09, 15A23

DOI. 10.1137/120865574

1. Introduction.

Modeling of two-phase immiscible flows in porous media is important for many industrial applications, such as oil recovery [12] and carbon sequestration [1]. Mathematical conceptualizations for such flows include the Buckley–Leverett model, which, in its simplest form, is represented by a nonlinear advection equation [4] for the relative saturation of fluid phases. Parameterizations of these flow equations are complicated by the multiscale heterogeneity and incomplete characterization of typical porous media. Consequently, many parameters in the governing equations exhibit a high degree of uncertainty, and quantification of predictive uncertainty becomes paramount. It is common to represent parametric uncertainty in probabilistic terms by treating uncertain parameters as (correlated) random fields. This renders otherwise deterministic governing equations stochastic. Their complete solutions are given by a probabilistic density function (PDF) or cumulative density function (CDF) of dependent variables.

Several conceptual frameworks have been proposed to solve stochastic differential equations describing two-phase immiscible flow in heterogeneous porous media with uncertain properties. One of them is Monte Carlo simulation (MCS), in which multiple (equally likely) realizations of random parameters serve as inputs for the corresponding deterministic governing equations. A statistical postprocessing is then conducted to obtain the distribution (histograms) of dependent variables. While MCSs are very robust and easy to implement, they have high computational costs due to their slow

*Received by the editors February 10, 2012; accepted for publication (in revised form) September 20, 2012; published electronically January 15, 2013. This work was supported by the Office of Advanced Scientific Computing Research funded by the U.S. Department of Energy. Pacific Northwest National Laboratory is operated by Battelle for the U.S. Department of Energy under contract DE-AC05-76RL01830. The U.S. Government retains a nonexclusive, royalty-free license to publish or reproduce the published form of this contribution, or allow others to do so, for U.S. Government purposes. Copyright is owned by SIAM to the extent not limited by these rights.
http://www.siam.org/journals/mms/11-1/86557.html

†Pacific Northwest National Laboratory, Richland, WA 99352 (Peng.Wang@pnnl.gov, kj@pnnl.gov, alexandre.tartakovsky@pnnl.gov).

‡Department of Mechanical and Aerospace Engineering, University of California, San Diego, La Jolla, CA 92093 (dmt@ucsd.edu).

convergence rate (inversely proportional to the square root of the number of realizations). Alternatives to MCS include derivation of deterministic equations for leading statistical moments of the system states [10, 13, 30, 22, 23, 24, 29, 28] and polynomial chaos expansions [6, 9, 16, 15, 17].

The first two statistical moments (ensemble mean and variance) can be used to forecast a system's average response and to measure an associated prediction error, respectively. These statistics are insufficient for risk assessment [25], where one is typically concerned with the probability of rare events. The use of PDF methods [20] for uncertainty quantification [14, 26, 27] addresses this need by deriving deterministic equations for PDFs of the system states. The PDF methods, as well as the moment equation methods, require a closure that is problem dependent. To our knowledge, no closures (and computable deterministic equations) exist for PDFs of nonlinear stochastic advection equations. Equally important, formulation of boundary conditions for PDF equations is not unique.

We propose an alternative CDF method for the stochastic Buckley–Leverett equation. In section 2 we describe the CDF method. In section 3 we derive a general deterministic equation for the (single-point) CDF of saturation. In section 4 we provide a semianalytical solution for the CDF of saturation in one spatial dimension. Discussion of the main features of the semianalytical solution and its comparison with MCS results are provided in section 5. The final conclusions are given in section 6.

2. Problem formulation. Darcy's law provides a macroscopic description of multiphase flow in porous media. An example of two-phase flows, which is of interest for secondary oil recovery, is oil (o) being displaced by water (w) in a reservoir with intrinsic permeability κ and porosity ϕ. For horizontal flow with negligible capillary pressure, Darcy's law takes the form

$$\mathbf{q}_w = -\kappa \frac{\kappa_{rw}}{\mu_w} \nabla p, \qquad \mathbf{q}_o = -\kappa \frac{\kappa_{ro}}{\mu_o} \nabla p, \tag{2.1}$$

where $\mathbf{q}_w$ and $\mathbf{q}_o$ denote Darcy fluxes of the wetting (water) and nonwetting (oil) phases, respectively; κ_{ri} and μ_{ri} are relative permeability and viscosity of a given fluid phase $i = \{w, o\}$; and ∇p is the pressure gradient.

Let $V_w(\mathbf{x}, t)$ and $V_o(\mathbf{x}, t)$ denote the volumes of water and oil within an averaging volume centered at $\mathbf{x}$. Then water saturation $s(\mathbf{x}, t)$ of the averaging volume is defined as $s(\mathbf{x}, t) = V_w(\mathbf{x})/[V_w(\mathbf{x}, t) + V_o(\mathbf{x}, t)]$. Combining Darcy's law (2.1) with mass conservation of each phase yields the Buckley–Leverett equation [4],

$$\frac{\partial s}{\partial t} + \nabla \cdot \left(\frac{\mathbf{q}}{\phi} f_w(s) \right) = 0, \quad \mathbf{x} \in \Omega, \quad t > 0, \tag{2.2}$$

which is defined at every point $\mathbf{x}$ of a spatial d-dimensional domain $\Omega \subset \mathbb{R}^d$. The total volumetric flux of water and oil, $\mathbf{q} = \mathbf{q}_w + \mathbf{q}_o$, satisfies the continuity equation for incompressible flow $\nabla \cdot \mathbf{q} = 0$. The quantity $f_w = q_w/(q_w + q_o)$ is referred to as the fractional flow of water. For constant porosity ϕ, (2.2) can be rewritten as

$$\frac{\partial s}{\partial t} + \mathbf{v}(s) \cdot \nabla s = 0, \qquad \mathbf{v}(s) \equiv \frac{\mathbf{q}}{\phi} \frac{\partial f_w}{\partial s}. \tag{2.3}$$

Supplemented with appropriate initial and boundary conditions, the Buckley–Leverett equation (2.3) provides a good approximation to actual saturation distributions for high flow rates [2].

3. CDF equation. Heterogeneity and data sparsity make $\kappa(\mathbf{x})$ uncertain. Combined with uncertainty in boundary conditions, this renders predictions of flow behavior uncertain. We represent this uncertainty by treating $\mathbf{q}(\mathbf{x}, t)$ in (2.3) as a random field with a known PDF. To solve the resulting stochastic Buckley–Leverett equation, we start by introducing a "raw" (or "fine-grained") CDF of water saturation s,

$$\Pi(\Theta; \mathbf{x}, t) = \mathcal{H}[\Theta - s(\mathbf{x}, t)], \tag{3.1}$$

where $\mathcal{H}$ is the Heaviside step function and Θ is a deterministic value (outcome) that the random water saturation s takes at a space-time point $(\mathbf{x}, t)$. Let $p_{\mathrm{s}}(\Theta; \mathbf{x}, t)$ denote the single-point PDF of water saturation s at point $(\mathbf{x}, t)$. Then the ensemble average of $\mathcal{H}$ over random s leads to the single-point CDF,

$$\langle \Pi(\Theta; \mathbf{x}, t) \rangle \equiv \int_{-\infty}^{\infty} \mathcal{H}(\Theta - s')\, p_{\mathrm{s}}(s'; \mathbf{x}, t)\, \mathrm{d}s' = F_s(\Theta; \mathbf{x}, t). \tag{3.2}$$

For smooth solutions of (2.3), their raw CDF satisfies a linear stochastic linear hyperbolic equation (see Appendix A)

$$\frac{\partial \Pi}{\partial t} + \mathbf{v}(\Theta) \cdot \nabla \Pi \;=\; 0, \quad \mathbf{x} \in \Omega, \quad t > 0, \tag{3.3}$$

subject to the initial condition

$$\Pi(\Theta; \mathbf{x}, t = 0) = \Pi_{\mathrm{in}} = \mathcal{H}\left[\Theta - s_{\mathrm{in}}(\mathbf{x})\right], \tag{3.4}$$

and appropriate boundary conditions in the physical domain Ω. Derivation of an equation corresponding to (3.3) for discontinuous solutions has to account for shock (e.g., entropy) conditions. It may lead to the presence of additional "kinetic defect" terms in (3.3) [18, 19]. Further study is needed to extend the deterministic analyses [18, 19] to the derivation of CDF equations in two and three spatial dimensions. For discontinuous solutions in one spatial dimension, shocks can be explicitly resolved (for each random realization) to bypass the need for the more general equation containing a kinetic defect term. In the example in section 4 we pursue the latter approach.

The raw CDF formulation (3.3) offers a number of advantages over direct solutions of the flow equations (2.3). First, for overall uncertainty quantification, one needs to compute (e.g., with MCS or stochastic finite elements) only the first ensemble moment of Π to obtain the full single-point CDF of s. Second, linearity of the raw CDF equation (3.3) facilitates its theoretical and numerical analyses. More important for the subsequent analysis, one can take advantage of the large body of literature on stochastic averaging of linear advective transport in random velocity fields $\mathbf{v}(\mathbf{x}, t)$. Specifically, the ensemble averaging of (3.3) yields an effective transport equation for the CDF of s [33],

$$\frac{\partial F_s}{\partial t} + \mathbf{v}_{\mathrm{eff}} \cdot \nabla_4 F_s = \nabla_4 \cdot (\mathbf{D} \nabla_4 F_s), \quad (\Theta, \mathbf{x}) \in [0, 1] \times \Omega, \quad t > 0, \tag{3.5}$$

where $\mathbf{v}_{\mathrm{eff}}$ is the $(d+1)$-dimensional "effective velocity," $\mathbf{D}$ is the $(d+1)$-dimensional eddy-diffusivity second-order tensor, and $\nabla_4 = (\partial/\partial x_1, \ldots, \partial/\partial x_d, \partial/\partial \Theta)^{\top}$ is the $(d+1)$-dimensional del operator. This equation is based on a closure approximation, but it is asymptotically exact for a particular formulation of $\mathbf{v}_{\mathrm{eff}}$ and $\mathbf{D}$ when F_s varies slowly with $\mathbf{x}$ and t relative to $\mathbf{v}$ [11].

Boundary conditions for $F_s(\Theta; \mathbf{x}, t)$ at $\Theta = 0$ and 1 are formulated in a straightforward and unambiguous manner: $F_s(0; \mathbf{x}, t) = 0$ and $F_s(1; \mathbf{x}, t) = 1$. This provides a key advantage of our CDF method over commonly used PDF equations [20], since the corresponding boundary conditions for PDF are not uniquely defined.

4. One-dimensional Buckley–Leverett problem. To simplify the presentation of the CDF method, we restrict the subsequent analysis to the one-dimensional problem on the domain $\Omega = [0, \infty)$. We assume that initially the domain is mostly saturated with oil and has a small uniform (irreducible) water saturation s_{wi},

$$s(x, t = 0) = s_{in} = s_{wi}. \tag{4.1}$$

Furthermore, we consider the boundary condition

$$s(x = 0, t) = s_0 = 1 - s_{oi}, \tag{4.2}$$

where s_{oi} is the irreducible oil saturation. This boundary condition represents injection of water at the boundary $x = 0$ into an initially oil-saturated field ($s_{in} = s_{wi}$). In the following, s_{oi} and s_{wi} are treated as deterministic constants, but they may in general be modeled as random variables.

In $d = 1$ spatial dimensions, $\mathbf{v}(s)$ in (2.3) reduces to

$$v(s) = \frac{q}{\phi} \frac{\partial f_w}{\partial s}. \tag{4.3}$$

The general continuity equation, $\nabla \cdot \mathbf{q} = 0$, now requires the total flux q to be constant in x and equal to the injection flow rate $q(x, t) = q(x = 0, t) = q_0(t)$. We allow the flow rate $q_0(t)$ to be uncertain, i.e., treat it as a random field with a prescribed PDF.

Combining the one-dimensional versions of Darcy's law (2.1) yields an expression for the fractional flow of water

$$f_w = \frac{q_w}{q_w + q_o} = \frac{\kappa_{rw}\mu_o}{\kappa_{rw}\mu_o + \kappa_{ro}\mu_w}. \tag{4.4}$$

A number of empirical constitutive models have been proposed to express relative permeabilities as functions of water saturation s. To be concrete, we adopt the Brooks–Corey quadratic relation [3]

$$\kappa_{rw} = \left(\frac{s - s_{wi}}{1 - s_{wi} - s_{oi}} \right)^2, \qquad \kappa_{ro} = \left(\frac{1 - s - s_{oi}}{1 - s_{wi} - s_{oi}} \right)^2. \tag{4.5}$$

Combining (4.3) and (4.4) yields

$$v(s) = \frac{2q\,(1 - s - s_{oi})\,(s - s_{wi})\,(1 - s_{oi} - s_{wi})\,\mu_o\mu_w}{\phi \left[(s - s_{wi})^2 \mu_o + (1 - s - s_{oi})^2 \mu_w \right]^2}. \tag{4.6}$$

4.1. Discontinuity in deterministic solution. For a given q, (2.3) can be solved using the method of characteristics, in which characteristic curves are defined according to $\mathrm{d}x/\mathrm{d}t = v(s)$ in the (x, t) plane. If $v(s)$ were monotonic, there would exist a one-to-one correspondence between the characteristics and the solution. The nonmonotonicity of $v(s)$ in (4.6) can cause different characteristic curves to intersect in finite time (Figure 4.1). This requires one to impose jump conditions, allowing for physically meaningful discontinuous (shock) solutions [2]. A water-oil discontinuous front at $x = x_f$ forms immediately and propagates in time with velocity $\mathrm{d}x_f/\mathrm{d}t$. Ahead (to the left) of the front, a rarefaction wave follows well-defined characteristic curves. Behind (to the right of) the front, the saturation remains at the initial value, $s^+ = s_{wi}$.

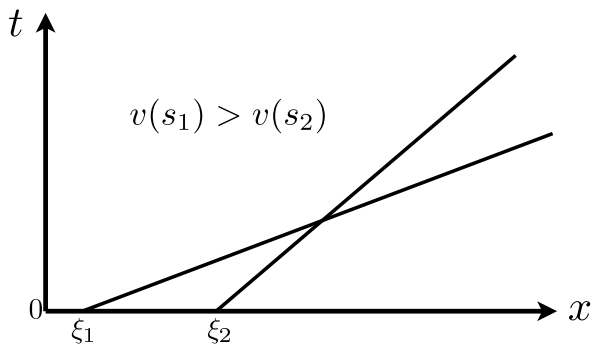

FIG. 4.1. *Illustration of intersecting characteristics for nonlinear first-order hyperbolic equation* (2.3) *when* $\mathrm{d}v/\mathrm{d}x < 0$.

The Rankine–Hugoniot condition at the discontinuity [21] defines the front location (and the saturation values ahead of the front) as

$$\frac{\mathrm{d}x_f}{\mathrm{d}t} = \frac{q}{\phi}\,\frac{f_w(s^-) - f_w(s^+)}{s^- - s^+}. \tag{4.7}$$

The saturation value ahead of the front, s^-, is constant along the characteristic curve defined by $\mathrm{d}x/\mathrm{d}t = v(s^-) = q/\phi\,(\mathrm{d}f_w/\mathrm{d}s)\,|_{s=s^-}$, which must match the shock speed:

$$\frac{f_w(s^-) - f_w(s^+)}{s^- - s^+} = \frac{\mathrm{d}f_w}{\mathrm{d}s}(s = s^-). \tag{4.8}$$

Solving (4.8) gives s^- and hence the location of shock front $x_f(t)$.

The continuous solution $s_r(x,t)$ ahead of the front (rarefaction) satisfies the Buckley–Leverett equation (2.3). It is found by using the method of characteristics in the range $s^- \le s_r \le 1 - s_{oi}$. The complete solution is then given by

$$s(x,t) = \begin{cases} s_r(x,t), & 0 \le x < x_f(t), \\ s_{wi}, & x > x_f(t). \end{cases} \tag{4.9}$$

Physically, it represents an oil-saturated zone to the right of the sharp water-oil front, with a smoothly varying mix of water and oil from the injection point to the left of the front. Other initial and boundary conditions can give rise to more complicated shock structures.

4.2. Solution for raw CDF. While the Buckley–Leverett equation is highly nonlinear, the raw CDF equation (3.3) is linear. Its one-dimensional version is

$$\frac{\partial \Pi}{\partial t} + v(\Theta)\frac{\partial \Pi}{\partial x} = 0, \tag{4.10a}$$

where

$$v(\Theta) = \frac{2q\,(1 - \Theta - s_{oi})\,(\Theta - s_{wi})\,(1 - s_{oi} - s_{wi})\,m}{\phi\left[(\Theta - s_{wi})^2 + (1 - \Theta - s_{oi})^2\,m\right]^2}, \qquad m = \frac{\mu_w}{\mu_o}. \tag{4.10b}$$

Thus, one would not expect the raw CDF to have any shock-like discontinuities. This may seem somewhat paradoxical considering our previous argument for saturation discontinuity in the physical space.

However, this discontinuity of s in the physical space translates into a discontinuity of the CDF (and the PDF) of s in the space of Θ. To be specific, the raw CDF $\Pi(\Theta; x, t)$ in (3.1) is subdivided into two parts, Π_a and Π_b, according to the saturation solution (4.9), as

$$\Pi(\Theta, x, t) = \begin{cases} \Pi_a = \mathcal{H}(\Theta - s_{wi}), & \Theta < s^-, \quad x > x_f(t), \\ \Pi_b = \mathcal{H}(\Theta - s_r), & s^- < \Theta, \quad x < x_f(t). \end{cases} \tag{4.11a}$$

For the example considered here, the rarefaction solution $s_r(x, t)$ is easy to obtain. This solution would also provide a direct mapping of parametric uncertainty onto system state uncertainty [31, 32]. This would render the introduction of Π redundant. However, in most cases (and certainly for the Buckley–Leverett equation in higher dimensions) analytical solutions are a rarity. This is the *raison d'être* for the CDF method developed here.

In (4.11a), Π_a is independent of either x or t, while Π_b satisfies the one-dimensional raw CDF equation (4.10). We show in Appendix B that

$$\Pi_b = \mathcal{H}(\Theta - 1 + s_{oi})\mathcal{H}(C - x) + \mathcal{H}(\Theta - s_{wi})\mathcal{H}(x - C), \tag{4.11b}$$

where $C(\Theta, t) = \int_0^t v(\Theta, t')\,\mathrm{d}t'$.

4.3. Solution for CDF. In accordance with (3.2), the saturation CDF is obtained by taking the ensemble average of Π in (4.11). Since both saturation and shock location are random, the ensemble average is formally given by

$$F_s(\Theta; x, t) = \int_{-\infty}^{\infty}\int_{-\infty}^{\infty} \Pi_a \mathcal{H}(x - x_f) p^+_{s,x_f}(s', x_f; x, t)\mathrm{d}s'\mathrm{d}x_f \tag{4.12a}$$

for $\Theta < s^-$ and by

$$\begin{aligned} F_s(\Theta; x, t) = & \int_{-\infty}^{\infty}\int_{-\infty}^{\infty} \Pi_a\, \mathcal{H}(x - x_f)\, p^+_{s,x_f}(s', x_f; x, t)\mathrm{d}s'\mathrm{d}x_f \\ & + \int_{-\infty}^{\infty}\int_{-\infty}^{\infty} \Pi_b\, \mathcal{H}(x_f - x)\, p^-_{s,x_f}(s', x_f; x, t)\mathrm{d}s'\mathrm{d}x_f \end{aligned} \tag{4.12b}$$

for $\Theta \geq s^-$. Here p_{s,x_f} denotes the (unknown) joint PDF of saturation and front location, while the superscripts $^-$ and $^+$ indicate the component of this PDF restricted to values of saturation before and after the front, respectively, for a given x and t. The first term in (4.12b) is required because the CDF is a cumulative probability. This CDF expression may be generalized to account for multiple shocks by considering multiple jump conditions and rarefaction zones according to the theory of hyperbolic conservation laws [21]. This generalization will be studied in the future; here we continue to focus on the case with $s(x, 0) = s_{wi}$ and $s(0, t) = 1 - s_{oi}$.

5. Computational example. We solve (4.11) for a time-dependent statistically homogeneous random flux $q(t)$ that has a lognormal distribution $p_q(Q)$ with mean μ_q and variance σ_q^2 and that exhibits an exponential correlation structure with correlation time τ_q. The flux is imposed at $x = 0$ and regarded as the system's sole source of uncertainty.

5.1. Nondimensionalization. The statistics μ_q and τ_q introduce a characteristic velocity and a characteristic time scale, respectively. Furthermore, we define a characteristic length scale L as

$$L = \mu_q \tau_q. \tag{5.1}$$

This gives rise to dimensionless quantities

$$x^\star = \frac{x}{L}, \quad x_f^\star = \frac{x_f}{L}, \quad t^\star = \frac{t}{\tau_q}, \quad C^\star = \frac{C}{L}, \quad Q^\star = \frac{Q}{\mu_q}. \tag{5.2}$$

The superscript * is omitted in the following to simplify the representation.

5.2. Results and discussion. Uncertainty in the boundary flux $q_0(t)$ gives rise to uncertainty (randomness) in saturation and shock location. The PDF of the former is related to the joint PDF of the latter by $p_{s,x_f}\mathrm{d}s'\mathrm{d}x_f = p_q \mathrm{d}Q$. The saturation CDF (4.12) becomes

$$F_s(\Theta; x, t) = \begin{cases} \int_{-\infty}^{\infty} \Pi_a \, \mathcal{H}(x - x_f) p_q \mathrm{d}Q, & \Theta < s^-, \\ \int_{-\infty}^{\infty} \left[\Pi_a \mathcal{H}(x - x_f) + \Pi_b \mathcal{H}(x_f - x)\right] p_q \mathrm{d}Q, & \Theta \geq s^-. \end{cases} \tag{5.3}$$

The (non-Gaussian, correlated) random field $q(t)$ enters (4.11) and, hence, (5.3) only as an integrand in

$$C(\Theta, t) = \int_0^t v(\Theta, t')\,\mathrm{d}t' = \frac{1}{\phi} \frac{\partial f_w(\Theta)}{\partial \Theta} \int_0^t q(t')\,\mathrm{d}t'. \tag{5.4}$$

Let

$$I_q(t) = \int_0^t q(t')\mathrm{d}t'. \tag{5.5}$$

Then (5.3) is transformed into

$$F_s(\Theta; x, t) = \begin{cases} \int_{-\infty}^{\infty} \Pi_a \mathcal{H}(x - x_f) p_{I_q} \mathrm{d}I, & \Theta < s^-, \\ \int_{-\infty}^{\infty} \left[\Pi_a \mathcal{H}(x - x_f) + \Pi_b \mathcal{H}(x_f - x)\right] p_{I_q} \mathrm{d}I, & \Theta \geq s^-, \end{cases} \tag{5.6}$$

where $p_{I_q}(I; t)$ is the PDF of $I_q(t)$. Based on the correlation time τ_q, we subdivide the temporal evolution of F_s into three periods with three different approximation schemes.

For small times, $t \ll \tau_q$, the flux $q(t')$ on the interval $[0, t]$ is approximately constant, $I_q \approx qt$, and $C(\Theta, t)$ can be approximated by

$$C(\Theta, t) \approx \frac{2qt(1 - \Theta - s_{oi})(\Theta - s_{wi})(1 - s_{oi} - s_{wi})m}{\phi[(\Theta - s_{wi})^2 + (1 - \Theta - s_{oi})^2 m]^2}, \quad t \ll \tau_q. \tag{5.7}$$

For large times, $t \gg \tau_q$, a white-noise (WN) approximation is appropriate, so that $I_q(t)$ is approximately Gaussian with mean $t\mu_q$ and variance $2t\sigma_q^2$. Then

$$C(\Theta, t) \approx \frac{2(1 - \Theta - s_{oi})(\Theta - s_{wi})(1 - s_{oi} - s_{wi})m}{\phi[(\Theta - s_{wi})^2 + (1 - \Theta - s_{oi})^2 m]^2} N(t\mu_q, 2t\sigma_q^2), \quad t \gg \tau_q. \tag{5.8}$$

In some applications (see, e.g., [5]), $q(t)$ lacks temporal correlation, and this expression becomes exact.

For intermediate times, we approximate the statistics of $I_q(t)$ with the central limit theorem (CLT)-based approach [7, 8, 34] outlined in Appendix C.

In the following sections, we first examine the accuracy and robustness of the alternative approximations of $p_{I_q}(I;t)$ by comparing them with the MCS performed on the shock solution (4.7)–(4.9). Next, we present and discuss both temporal and spatial profiles of the saturation CDF F_s. Finally, we investigate the impact of the degree of uncertainty in the boundary flux $q(t)$ on the saturation CDF. Unless specified otherwise, the following simulations correspond to lognormal distribution of boundary flux with mean $\mu_q = 1$ and standard deviation $\sigma_q = 0.5$, flux correlation time $\tau_q = 1$, and irreducible water and oil saturation $s_{wi} = s_{oi} = 0.1$. The ratio of relative viscosities is set to $m = 0.01$.

5.2.1. Model validation and verification. Here we validate the CDF equation (5.3) and verify the accuracy of its numerical solution. To validate the CDF equation, we compare its solution in the limit of $\sigma_q = 0$ with the solution of the deterministic Buckley–Leverett equation (4.9) with $q = \mu_q$. In this limit, the PDF of q becomes $p_q(Q) = \delta(Q - \mu_q)$ and the CDF equation (5.3) reduces to

$$F_s(\Theta;x,t) = \begin{cases} \mathcal{H}(\Theta - s_{wi})\mathcal{H}(x - x_f), & \Theta < s^-, \\ \mathcal{H}(\Theta - s_{wi})\mathcal{H}(x - x_f) + \mathcal{H}(x_f - x)\left[\mathcal{H}(C - x)\right. & \\ \quad \left. \times\, \mathcal{H}(\Theta - 1 + s_{oi}) + \mathcal{H}(x - C)\mathcal{H}(\Theta - s_{wi})\right], & \Theta \geq s^-. \end{cases} \tag{5.9}$$

For a given x and t, the solution of the deterministic Buckley–Leverett equation is given by the value of Θ at which F_s undergoes a jump from 0 to 1. For $x < x_f$, the saturation value at point (x,t) is given by the solution of the equation $C(\Theta,t) = x$ for $s = \Theta$ and, for $x > x_f$, the saturation is given by $s = s_{wi}$. This is equivalent to the solution (4.9) for the deterministic case.

To verify our CDF model, we compare its solution $F_s(\Theta;x,t)$ with that obtained with the MCS of the shock solution (section 4.1). These MCSs consist of computing multiple realizations of the random integral I_q,

$$F_s(\Theta;x,t) = P(I \leq I_1) = \int_0^{I_1} p_{I_q}(I)\mathrm{d}I, \qquad \Theta < s^-, \tag{5.10a}$$

$$F_s(\Theta;x,t) = P(I_1 < I \leq I_2) = \int_{I_1}^{I_2} p_{I_q}(I)\mathrm{d}I, \qquad \Theta \geq s^-, \tag{5.10b}$$

where $s^- = s_{wi} + (1 - s_{wi} - s_{oi})\sqrt{m/(m+1)}$ and

$$I_1 = \frac{\phi x}{\frac{\partial f_w}{\partial s}(s = s^-)}, \qquad I_2(\Theta) = \frac{\phi x}{\frac{\partial f_w}{\partial s}(s = \Theta)}. \tag{5.10c}$$

Figure 5.1 exhibits $F_s(\Theta)$ computed alternatively with the MCS and the CDF solution (5.3) under the three approximations of I_q. As time increases, the accuracy of both the CLT approximation and the WN approximation (5.8) improves, whereas that of the random constant approximation (5.7) (Const) deteriorates. For $t \leq \tau_q$ ($t = 0.1$, $t = 1$), the Const scheme provides a good estimate of the random integral I_q. At intermediate times ($t = 10$), the CLT and WN approximations agree well with

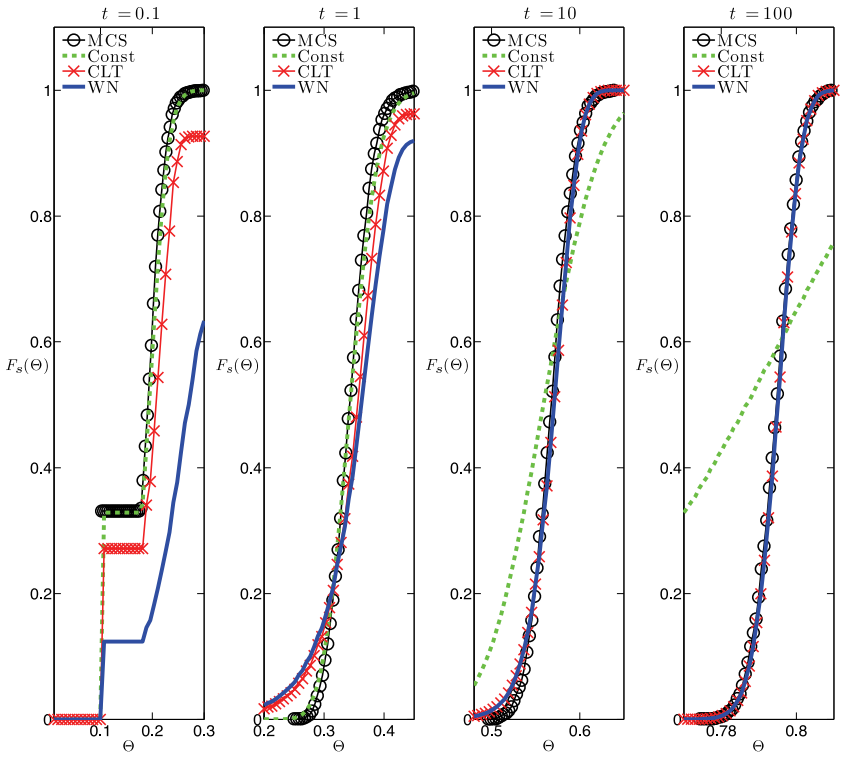

FIG. 5.1. *Saturation CDF $F_s(\Theta; x = 1, t)$ computed at four dimensionless times $t = 0.1$, $t = 1$, $t = 10$, and $t = 100$. These solutions are obtained with the MCS and the CDF solution* (5.3) *under the three alternative approximations: the random constant approximation* (5.7) *(Const), the CLT-based approximation (CLT), and the WN approximation* (5.8) *(WN). Only the portion of the domain in which the CDF varies is shown.*

the MCS, though the former has a slight edge. At later times ($t = 100$), the CLT and WN approximations are equally accurate. The WN approximation can be seen as an extension of the CLT approximation at large times (Appendix C).

5.2.2. Temporal evolution of saturation CDF. Four temporal snapshots of the saturation CDF $F_s(\Theta; x = 1, t)$ at dimensionless times $t = 0.01$, $t = 0.1$, $t = 10$, and $t = 100$ are shown in Figure 5.2. At early times ($t = 0.01$), the saturation is nearly deterministic, i.e., close to its initial (deterministic) value $s = s_{wi}$, which corresponds to an approximate step-function CDF. As time increases, the fluctuations associated with the random boundary flux $q_0(t)$ propagate along with the wetting front, increasing uncertainty in the predictions of the saturation profile at $t = 0.1$ and $t = 10$. As time elapses ($t = 10$), the front moves to the right of the observation point $x = 1$ in almost all realizations and F_s follows almost entirely a distribution of the rarefaction solution. Eventually ($t = 100$) the effect of random flux $q_0(t)$ diminishes and F_s approaches the Heaviside function representative of deterministic (known with certainty) predictions.

5.2.3. Spatial profiles of saturation CDF. Figure 5.3 shows the saturation CDF at dimensionless points $x = 0.01$, $x = 0.5$, $x = 50$, and $x = 500$ at fixed time

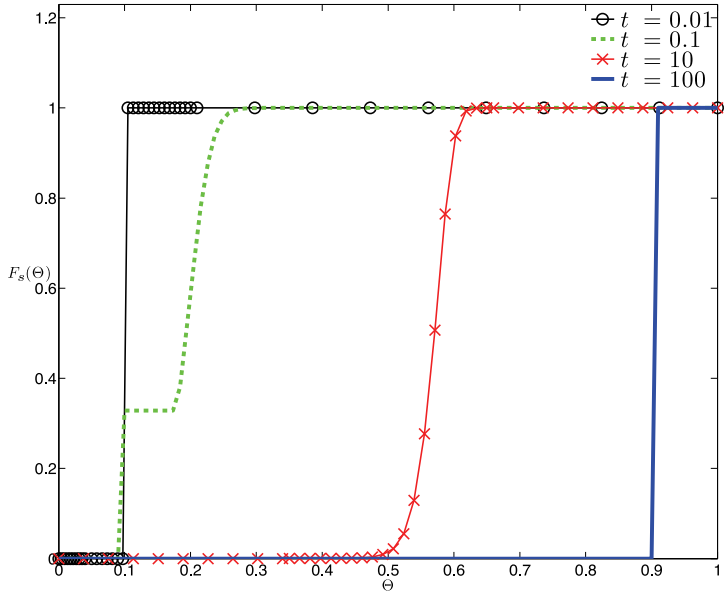

FIG. 5.2. *Temporal snapshots of the saturation CDF,* $F_s(\Theta; x = 1, t)$*, at four dimensionless times* $t = 0.01$*,* $t = 0.1$*,* $t = 10$*, and* $t = 100$*.*

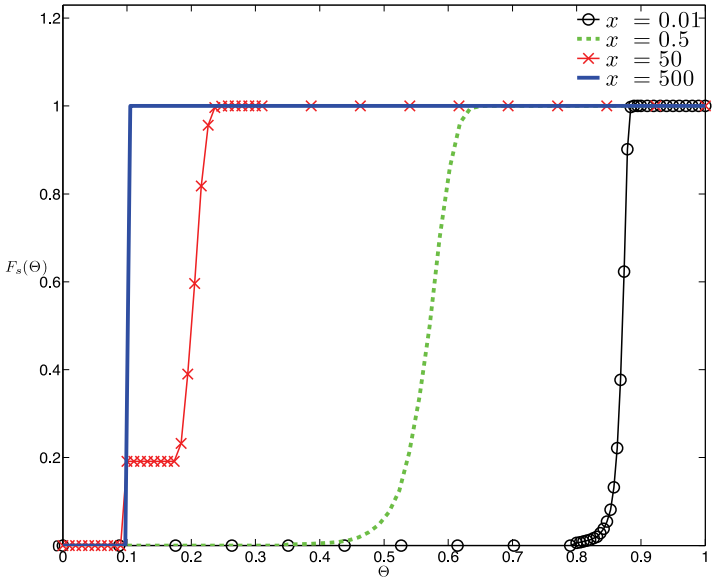

FIG. 5.3. *Saturation CDF,* $F_s(\Theta; x, t)$*, at* $t = 5$ *and four dimensionless locations* $x = 0.01$*,* $x = 0.5$*,* $x = 50$*, and* $x = 500$*.*

$t = 5$. The saturation CDF exhibits the same pattern as the temporal evolution does, but in reverse order. At $x = 0.01$, very few realizations have a saturation value below

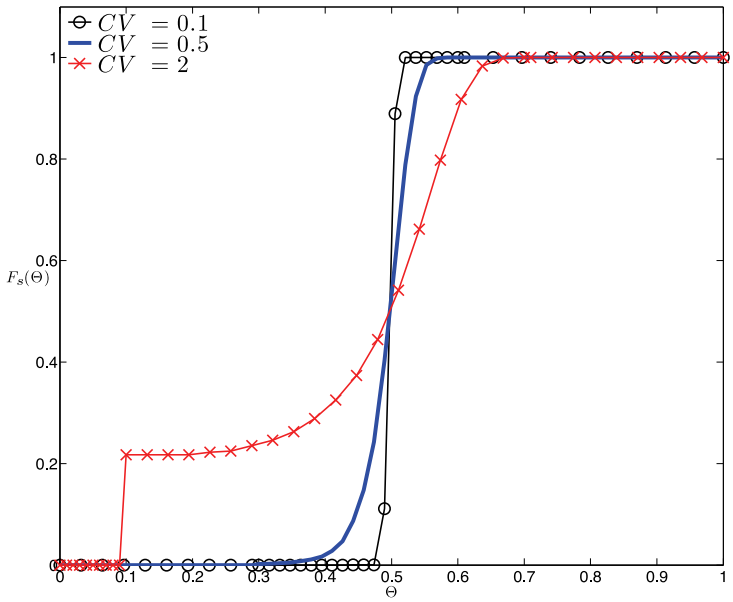

FIG. 5.4. *Saturation CDF, $F_s(\Theta; x = 1, t = 5)$, for three coefficients of variation of the boundary flux, $CV = 0.1$, $CV = 0.5$, and $CV = 2$.*

those in the upper range of the rarefaction zone. A significant portion of realizations have the front near $x = 0.5$, as indicated by the shape of the CDF at that x value. At $x = 500$, ahead of almost all realizations of the front, the medium maintains its initial saturation, as indicated by the Heaviside function shape of the CDF; behind the front, the medium is either partially saturated ($x = 0.5$) or fully saturated ($x = 0.01$).

5.2.4. Effect of degree of uncertainty on concentration CDF. The degree of the boundary flux uncertainty is encapsulated in the coefficients of variation, $CV = \sigma_q/\mu_q$. Figure 5.4 demonstrates its impact on $F_s(\Theta; x = 1,\ t = 5)$ for $CV = 0.1$, $CV = 0.5$, and $CV = 2$. As expected, the small CV yields a saturation profile approaching the step function. With rising fluctuations ($CV = 0.5$), the shape of the saturation CDF gradually spreads, indicating higher predictive uncertainty.

6. Conclusions. We present a novel method for obtaining the CDF F_s of a state variable $s(\mathbf{x}, t)$ whose evolution is described by the stochastic Buckley–Leverett model (first-order hyperbolic equation) with a random time-dependent flux. This CDF method converts an original stochastic equation into a deterministic equation for the CDF of the system state, in which uncertain parameters and initial and boundary conditions are described as random variables. Here we considered a one-dimensional problem with a random correlated in time flux prescribed at the boundary of a semi-infinite domain. We demonstrated that F_s found from the CDF method compares favorably with its counterpart obtained by MCS. Our analysis leads to the following major conclusions:

1. CDF equations and their semianalytical solutions provide a full statistical description of system states and enable one to perform probabilistic risk assessment,

which is focused on rare events as characterized by the tails of probability distributions.

2. The CDF method allows one to derive an exact computable deterministic equation for the CDF of nonlinear advection equations such as the Buckley–Leverett equation. To our knowledge, this is the first method that results in computable equations for the CDF (or PDF) for the nonlinear hyperbolic conservation laws with shocks.

3. Our approach converts the original stochastic nonlinear equation into a deterministic equation for the system state's CDF without any approximations. It allows one to preserve the underlying physics, in particular shocks, in the final solution.

4. Uncertainty in the boundary flux has a significant impact on uncertainty in predictions of the system state (water saturation).

5. The present analysis relies on the existing rarefaction solution of the deterministic Buckley–Leverett equation. However, our general CDF framework is also applicable to problems that do not admit deterministic analytical solutions.

6. Our formulation of the CDF equations may be generalized to the case of multiple shocks by considering multiple jump conditions and rarefaction zones according to the theory of hyperbolic conservation laws.

7. Derivation of the CDF equations for higher-dimensional problems with shocks might benefit from the deterministic theory of "kinetic defects" [18, 19].

Appendix A. Derivation of stochastic equation for raw CDF. Our derivation of the CDF equations is closely related to the PDF equations in turbulence [20] and their applications for uncertainty quantification [26]. We express the spatial and temporal derivatives of $\Pi(\Theta; \mathbf{x}, t)$ as

$$\nabla\Pi = \frac{\partial\Pi}{\partial s}\nabla s = -\frac{\partial\Pi}{\partial\Theta}\nabla s, \qquad \frac{\partial\Pi}{\partial t} = \frac{\partial\Pi}{\partial s}\frac{\partial s}{\partial t} = -\frac{\partial\Pi}{\partial\Theta}\frac{\partial s}{\partial t}. \tag{A.1}$$

For smooth solutions, multiplying (2.3) by $\partial\Pi/\partial\Theta$ and using the first expression in (A.1) yields

$$\frac{\partial\Pi}{\partial t} + \mathbf{v}(s)\,\frac{\partial\Pi}{\partial\Theta}\cdot\nabla s \;=\; 0. \tag{A.2}$$

Since $\partial\Pi/\partial\Theta = \delta(\Theta - s)$, this yields

$$\frac{\partial\Pi}{\partial t} + \mathbf{v}(s)\,\delta(\Theta - s)\;\cdot\nabla s = 0. \tag{A.3}$$

Finally, recalling that $f(s)\delta(\Theta - s) = f(\Theta)\delta(\Theta - s)$, we rewrite (A.2) as

$$\frac{\partial\Pi}{\partial t} + \mathbf{v}(\Theta)\,\frac{\partial\Pi}{\partial\Theta}\cdot\nabla s \;=\; 0. \tag{A.4}$$

Combining (A.4) and the second expression in (A.1) leads to (3.3).

This derivation is appropriate for smooth solutions, but in general hyperbolic equations of discontinuous solutions may form. In one spatial dimension, solutions with a single shock may be obtained by directly analyzing shock propagation. To account for shocks and entropy conditions in higher dimensions it might be possible to build upon the deterministic analysis of "kinetic defects" [18, 19].

Appendix B. Analytical solution to one-dimensional CDF equation. We use the method of characteristics to solve the linear hyperbolic equation (4.10) subject

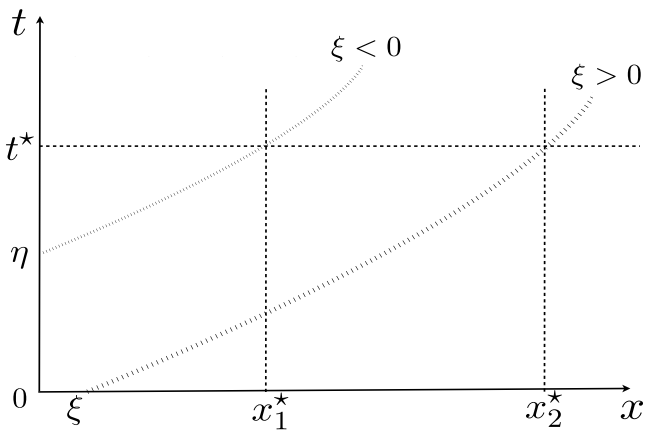

FIG. B.1. *Characteristic curves in the* (x,t) *plane for* $\Pi(Q;x,t)$.

to the following boundary and initial conditions:

$$\Pi(\Theta;x,t=0)=\mathcal{H}(\Theta-s_{wi}),\qquad \Pi(\Theta;x=0,t)=\mathcal{H}(\Theta-1+s_{oi}). \tag{B.1}$$

We derive a solution for the case in which the random velocity v is such that no shocks form in the underlying stochastic equation. This solution corresponds to a rarefaction zone when we consider a solution that does contain a shock. A family of characteristics, $x=x(t;\xi)$, is defined by

$$\frac{\mathrm{d}x}{\mathrm{d}t}=v(\Theta,x,t),\qquad x(t=0)=\xi, \tag{B.2}$$

where the "label" ξ defines the origin of each characteristic line (see Figure B.1). Its solution is

$$x=\int_0^t v(\Theta,x(t'),t')\mathrm{d}t'+\xi. \tag{B.3}$$

Along these characteristics, (4.10) becomes

$$\frac{\mathrm{d}\Pi}{\mathrm{d}t}=0, \tag{B.4}$$

which is to say that Π is a function of t and ξ only, i.e., $\Pi=g(t,\xi)$:

1. For $\xi\geq 0$, the characteristics originate from the x-axis ($t=0$) and the solution is determined by the boundary condition on t, i.e., by the initial condition in (B.1).

2. For $\xi<0$, the characteristics originate from the t-axis ($t=\eta$) and the solution is determined by the boundary condition on x. The variable η is a solution of $\int_0^\eta v\,\mathrm{d}t'=-\xi$.

Substituting (B.3) into (B.4), and eliminating ξ in favor of x and t in the solution, yields

$$\Pi = \mathcal{H}\left(\Theta - s_{wi}\right)\mathcal{H}(x - C) + \mathcal{H}\left(\Theta - 1 + s_{oi}\right)\mathcal{H}(C - x), \tag{B.5}$$

where $C = \int_0^t v(\Theta, x(t'), t')\,\mathrm{d}t'$.

Appendix C. Approximation of random integral I_q. For $t > \tau_q$, the statistics of the integral $I_q(t)$ in (5.5) can be computed with the methods presented in [7]. One starts by subdividing the integration interval $[0, t]$ into N subintervals of length $\Delta = t/N$. Then (5.5) is rewritten as

$$I_q(t) = \sum_{i=1}^{N} \chi_i = \sum_{i=1}^{N} \int_{(i-1)\Delta}^{i\Delta} q(t')\mathrm{d}t'. \tag{C.1}$$

Since $q(t)$ is a stationary process with a continuous sample function, the integrals χ_i $(i = 1, \ldots, N)$ share the same mean

$$\mu_\chi = \mu_q \Delta \tag{C.2}$$

and variance

$$\sigma_\chi^2 = \sigma_q^2 \int_{(i-1)\Delta}^{i\Delta} \int_{(i-1)\Delta}^{i\Delta} \rho_q(t' - t'')\mathrm{d}t'\mathrm{d}t'' = 2\sigma_q^2 \int_0^{\Delta} (\Delta - t')\rho_q(t')\mathrm{d}t'. \tag{C.3}$$

The two-point covariance between the intervals is given by

$$\mathrm{Cov}(\chi_1, \chi_i) = \sigma_q^2 \int_0^{\Delta} \int_{(i-1)\Delta}^{i\Delta} \rho_q(t' - t'')\mathrm{d}t'\mathrm{d}t'', \quad i \geq 2. \tag{C.4}$$

According to the CLT for correlated random variables [8, 34], $I_q(t) = \sum_{i=1}^{N} \chi_i$ is asymptotically (as $N \to \infty$) Gaussian with mean $N\mu_\chi$ and variance NV, where

$$V = \sigma_\chi^2 + 2\sum_{i=2}^{N} \mathrm{Cov}(\chi_1, \chi_i) < \infty. \tag{C.5}$$

For large times, $t \gg \tau_q$, this approximation is equivalent to the WN scheme in (5.8). This scheme fails when one considers small times, $t \ll \tau_q$, since the condition above (C.5) cannot be satisfied.

It is interesting to note that, as $N \to \infty$, the length of each interval tends to zero. In other words, $\Delta \ll \tau_q$, and hence the random field can be approximated as a random variable for each interval. Now (C.3) and (C.4) can be rewritten as

$$\sigma_\chi^2 = \sigma_q^2 \Delta^2, \tag{C.6}$$

$$\mathrm{Cov}(\chi_1, \chi_i) = \sigma_q^2 \Delta^2 \rho_q\left[(i-1)\Delta\right], \quad i \geq 2. \tag{C.7}$$

On the other hand, for $t \to \infty$, this approximation scheme is equivalent to that of white noise.

REFERENCES

[1] S. Bachu, *CO_2 storage in geological media: Role, means, status and barriers to deployment*, Prog. Energy Combust. Sci., 34 (2008), pp. 254–273.

[2] J. Bear, *Dynamics of Fluids in Porous Media*, Elsevier, New York, 1974.

[3] R. H. Brooks and A. T. Corey, *Hydraulic Properties of Porous Media: Hydrology Papers*, Colorado State University, Fort Collins, CO, 1964.
[4] S. E. Buckley and M. C. Leverett, *Mechanism of fluid displacement in sands*, Transactions of the AIME, 146 (1942), pp. 107–116.
[5] D. L. Buhman, T. K. Gates, and C. C. Watson, *Stochastic variability of fluvial hydraulic geometry: Mississippi and Red rivers*, J. Hydr. Engrg., 128 (2002), pp. 426–437.
[6] P. Cinnella and S. J. Hercus, *Robust optimization of dense gas flows under uncertain operating conditions*, Comput. & Fluids, 39 (2010), pp. 1893–1908.
[7] O. Ditlevsen, G. Mohr, and P. Hoffmeyer, *Integration of non-Gaussian fields*, Probab. Eng. Mech., 11 (1996), pp. 15–23.
[8] R. Durrett, *Probability: Theory and Examples*, Cambridge University Press, Cambridge, UK, 2010.
[9] R. Ghanem and S. Dham, *Stochastic finite element analysis for multiphase flow in heterogeneous porous media*, Transp. Porous Media, 32 (1998), pp. 239–262.
[10] K. D. Jarman and T. F. Russell, *Eulerian moment equations for* 2*-D stochastic immiscible flow*, Multiscale Model. Simul., 1 (2003), pp. 598–608.
[11] R. H. Kraichnan, *Eddy viscosity and diffusivity: Exact formulas and approximations*, Complex Systems, 1 (1987), pp. 805–820.
[12] L. Lake, *Enhanced Oil Recovery*, Prentice–Hall, Englewood Cliffs, NJ, 1989.
[13] P. Langlo and M. S. Espedal, *Macrodispersion for two-phase, immiscible flow in porous media*, Adv. Water Resour., 17 (1994), pp. 297–316.
[14] P. C. Lichtner and D. M. Tartakovsky, *Upscaled effective rate constant for heterogeneous reactions*, Stoch. Environ. Res. Risk Assess., 17 (2003), pp. 419–429.
[15] G. Lin and A. M. Tartakovsky, *An efficient, high-order probabilistic collocation method on sparse grids for three-dimensional flow and solute transport in randomly heterogeneous porous media*, Adv. Water Resour., 32 (2009), pp. 712–722.
[16] G. Lin and A. M. Tartakovsky, *Numerical studies of three-dimensional stochastic Darcy's equation and stochastic advection-diffusion-dispersion equation*, J. Sci. Comput., 43 (2010), pp. 92–117.
[17] G. Lin, A. M. Tartakovsky, and D. M. Tartakovsky, *Random domain decomposition for probabilistic collocation on sparse grids*, J. Comput. Phys., 229 (2010), pp. 6995–7012.
[18] P.-L. Lions, B. Perthame, and E. Tadmor, *A kinetic formulation of multidimensional scalar conservation laws and related equations*, J. Amer. Math. Soc., 7 (1994), pp. 169–191.
[19] B. Perthame, *Kinetic Formulation of Conservation Laws*, Oxford University Press, Oxford, UK, 2002.
[20] S. B. Pope, *Turbulent Flows*, Cambridge University Press, Cambridge, UK, 2000.
[21] J. Smoller, *Shock Waves and Reaction-Diffusion Equations*, Springer, New York, 1983.
[22] A. M. Tartakovsky, L. Garcia-Naranjo, and D. M. Tartakovsky, *Transient flow in a heterogeneous vadose zone with uncertain parameters*, Vadose Zone Journal, 3 (2004), pp. 154–163.
[23] A. M. Tartakovsky, P. Meakin, and H. Huang, *Stochastic analysis of immiscible displacement of the fluids with arbitrary viscosities and its dependence on support scale of hydrological data*, Adv. Water Resour., 27 (2004), pp. 1151–1166.
[24] A. M. Tartakovsky, S. P. Neuman, and R. J. Lenhard, *Immiscible front evolution in randomly heterogeneous porous media*, Phys. Fluids, 15 (2003), pp. 3331–3341.
[25] D. M. Tartakovsky, *Probabilistic risk analysis in subsurface hydrology*, Geophys. Res. Lett., 34 (2007), L05404.
[26] D. M. Tartakovsky and S. Broyda, *PDF equations for advective-reactive transport in heterogeneous porous media with uncertain properties*, J. Contam. Hydrol., 120–121 (2011), pp. 129–140.
[27] D. M. Tartakovsky, M. Dentz, and P. C. Lichtner, *Probability density functions for advective-reactive transport in porous media with uncertain reaction rates*, Water Resour. Res., 45 (2009), W07414.
[28] D. M. Tartakovsky, A. Guadanini, F. Ballio, and A. M. Tartakovsky, *Localization of mean flow and apparent transmissivity tensor for bounded randomly heterogeneous aquifers*, Transp. Porous Media, 49 (2002), pp. 41–58.
[29] D. M. Tartakovsky, Z. Lu, A. Guadagnini, and A. M. Tartakovsky, *Unsaturated flow in heterogeneous soils with spatially distributed uncertain hydraulic parameters*, J. Hydrol., 275 (2003), pp. 182–193.
[30] E. Teodorovich, P. Spesivtsev, and B. Nœtinger, *A stochastic approach to the two-phase displacement problem in heterogeneous porous media*, Transp. Porous Media, 87 (2011), pp. 151–177.

[31] P. Wang and D. M. Tartakovsky, *Probabilistic predictions of infiltration into heterogeneous media with uncertain hydraulic parameters*, Int. J. Uncert. Quant., 1 (2011), pp. 35–47.
[32] P. Wang and D. M. Tartakovsky, *Reduced complexity models for probabilistic forecasting of infiltration rates*, Adv. Water Resour., 34 (2011), pp. 375–382.
[33] P. Wang and D. M. Tartakovsky, *Uncertainty quantification in kinematic-wave models*, J. Comput. Phys., 231 (2012), pp. 7868–7880.
[34] H. White, *Asymptotic Theory for Econometricians*, Academic Press, New York, 2001.